

Conformation of Intramolecularly Cross-Linked Polymer Nanoparticles on Solid Substrates

Tiffany E. Dukette and Michael E. Mackay*

*Chemical Engineering and Materials Science, Michigan State University,
East Lansing, Michigan 48824*

Brooke Van Horn and Karen L. Wooley

*Department of Chemistry, Washington University—St. Louis,
St. Louis, Missouri 63130*

Eric Drockenmuller, Michael Malkoch, and Craig J. Hawker

*Materials Research Laboratory, University of California,
Santa Barbara, California 93106*

Received May 19, 2005; Revised Manuscript Received July 7, 2005

ABSTRACT

The conformation of cross-linked, monomolecular, polystyrene nanoparticles on a solid substrate is considered as a function of cross-linking degree and substrate surface free energy. It is found that an extreme amount of cross-linking is necessary for the ca. 5–10 nm diameter nanoparticles to retain their original spherical shape, regardless of surface free energy. A lesser amount of cross-linking produces a nanoparticle that collapses to a pancake-like conformation on a high-energy substrate yet remains spherical on a low-energy surface. A simple model is developed to reveal the relationship between nanoparticle modulus and surface free energy to define the nanoparticle conformation.

A recent advance in data storage technology is the Millipede¹ used to store information by pushing a hole into a polymer film with a heated atomic force microscopy (AFM) tip generating, in effect, two-dimensional ticker tape. Here we study a potential technology that is essentially the geometrical inverse of the Millipede. Polymer nanoparticles, arranged on a solid substrate, are individually addressed through plastic deformation with an AFM probe. Each nanoparticle represents a bit of information; i.e., “1” when deformed and a “0” in its initial state. We recognize the initial conformation of nanoparticles on solid substrates, prior to deformation, is dictated by their intrinsic rigidity and interaction with a substrate which represents a critical aspect of this technology.

To delineate the effect of rigidity and nanoparticle–substrate interaction, we study unique polystyrene nanoparticles synthesized by intramolecular cross-linking.² The rigidity is varied by the degree of cross-linking to produce extremely robust nanoparticles approximately 5–10 nm in size. Further, the substrate surface free energy is changed by choosing a high free energy surface, freshly cleaved mica, and a low free energy surface, silanized silicon wafer. Both substrates are smooth at the angstrom level thereby minimizing roughness effects on the measurements.

It should be noted that the conformation of larger organic nanoparticles on solid substrates has been studied before by determining how they change size upon heating.³ Also, in 1965, prior to present day atomic force microscopy, Richardson used scanning electron microscopy (SEM) to determine the molecular weight of individual molecules.⁴ Polystyrene solution was sprayed onto a carbon-backed mica substrate and shadowed with deposits of gold and palladium. The shadow length for each molecule could then be determined through SEM images. To calculate the molecular weight of the individual molecules, it was assumed that the particles were spherical and that the diameter of the particles was equal to their height. Due to limitations, there are two major difficulties in using this technique: defining the shadow limit cast by the spheres and the assumption of a spherical conformation on the substrate. Richardson used a precipitant/solvent solution to prevent molecules from collapsing, but he did not take into account surface free energy effects on the molecules. According to our results, un-cross-linked polymer molecules deform substantially even on a low-energy substrate, at least with our preparation procedure.

Polystyrene nanoparticles were synthesized according to a previously described procedure² demonstrated in Figure 1. Briefly a linear copolymer consisting of styrene monomer

* Corresponding author: mackay@msu.edu; www.nanoeverything.com.

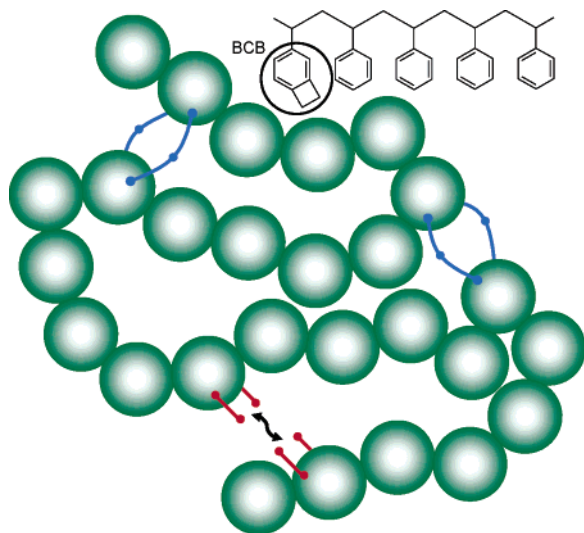


Figure 1. Intramolecular cross-linking of polystyrene macromolecules is accomplished by opening a pendent benzocyclobutene (BCB) group and subsequent reaction cross-linking with a similarly activated group. The molecule is representative of a tightly cross-linked nanoparticle with every fifth monomer unit potentially cross-linked.

Table 1. Sample, Molecular Mass, Polydispersity Index, Degree of Cross-Linking, Nature (i.e., linear precursor or cross-linked nanoparticle), and Diameter if the Molecules Collapse to the Bulk Density of Polystyrene (eq 1) for the Samples

sample	M_n (kDa)	PDI	mol % cross-linking agent	nature	diameter (nm)
PS33k	33.0	1.05	20	linear	4.7
PS58k	58.0	1.14	20	linear	5.6
PS193k	193	1.28	20	linear	8.4
L-PS25k	24.5	1.14	2.5	cross-linked	4.2
L-PS60k	60.1	1.16	2.5	cross-linked	5.7
L-PS158k	158	1.40	2.5	cross-linked	7.8
T-PS41k	41.0	1.04	20	cross-linked	5.0
T-PS78k	78.0	1.14	20	cross-linked	6.2
T-PS211k	211	1.32	20	cross-linked	8.6
E-PS33k	33.0	1.91	60	cross-linked	4.7

and styrene monomer containing a pendent cross-linking group (benzocyclobutene, BCB) was first synthesized. The degree of cross-linking was dictated by the BCB content and here we use three BCB levels: 2.5, 20, and 60 mol %, denoted as lightly (L), tightly (T), and extremely (E) cross-linked. A dilute solution of the linear precursor was then dripped into hot solvent activating the intramolecular cross-linking reaction to create nanoparticles containing a single macromolecule. The nanoparticle size is dictated by the initial precursor molecular weight and the degree of cross-linking. The sample codes, molecular weights (M_n , number average molecular weight), polydispersity index (PDI, ratio of weight to number average molecular weight), and degree of cross-linking for the systems studied here are given in Table 1. Note the molecular weights were determined with a Wyatt "Dawn EOS" 18 angle static light scattering detector, and so are absolutely measured and not relative to calibration

standards. Some slight aggregation of the linear precursors is suggested by these results.

Surface profile measurements were performed with a Pacific Nanotechnology Nano-R atomic force microscope in close contact (oscillating) mode to generate height images that were not altered other than a simple leveling procedure. Silicon tips with a spring constant of 36 N/m, tip curvature of 10–20 nm, and a resonance frequency of 286–339 kHz were used for all experiments.

Freshly cleaved mica and silanized silicon wafer substrates were used to determine the influence of surface free energy on the nanoparticle conformation. The cleaved mica surfaces were used immediately to avoid contamination from dust, atmospheric contaminants, and ionic crystals that are attracted to the surface due to mica's hydrophilic nature.⁵ Sigmacote was used to silanize the silicon wafers by spin coating the Sigmacote solution onto a silicon wafer at 5000 rpm for 40 s. Sigmacote (Sigma-Aldrich) is a solution consisting of 2.5% chlorosiloxane ((SiCl₂C₄H₉)₂O) and 97.5% heptane that functionalizes the surface with short alkane chains. The wafer was rinsed with Millipore water to eliminate the excess, and then pure benzene was spin coated directly onto the wafer leaving only a monolayer. The silanized wafer was then checked by AFM to ensure the coating provided a smooth surface containing no precipitates or dust particles.

The linear polymer precursors and nanoparticles were dissolved in benzene, and all solutions were filtered with a 0.2 μ m Teflon filter to reduce the amount of large dust particles and atmospheric contaminants. The solutions (concentration, 1–5 μ g/mL) were spin coated at 5000 rpm for 40 s on the mica substrate. Due to Sigmacote's extremely low free energy surface (29 mN/m), the solutions could not be spin coated directly onto the surface and therefore a drop of solution (concentration, 0.01 μ g/mL) was placed on the surface and exposed to air until the benzene had completely evaporated. We tried other preparation procedures similar to what Richardson suggested⁴ and found minimal differences in the height values discussed below suggesting the solvent and preparation procedure do not significantly affect the results, at least for the solvents we have tried.

The nanoparticle heights were determined with AFM by taking the average of 50 particle heights; however, the lateral size could not be found due to convolution effects created by the tip.^{6,7} In Figure 2 an example of three-dimensional AFM height image of the T-PS211k nanoparticles on the mica and Sigmacote substrates is shown. The images clearly demonstrate a uniformity of nanoparticles on the surfaces and the narrow height distribution provides evidence that only individual polystyrene nanoparticles are present and no agglomeration of nanoparticles occurs.

To ascertain the nanoparticle conformation on the substrate shown in Figure 2, we determine the diameter (D) assuming the macromolecule collapses to a sphere with the bulk density of polystyrene ($\rho = 1.04$ g/cm³) through

$$D = \left[\frac{6M_n}{\pi N_A \rho} \right]^{1/3} \quad (1)$$

where N_A is Avogadro's number. The values are given in

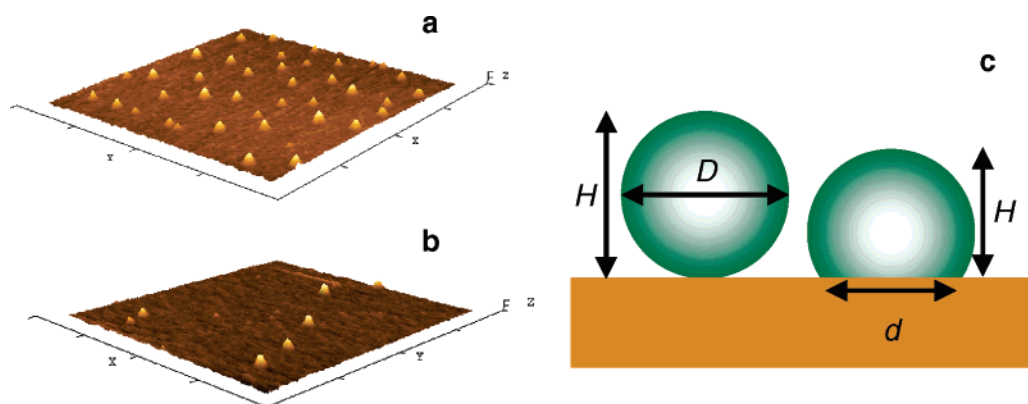


Figure 2. (a) Atomic force microscopy height images of T-PS211k polystyrene nanoparticles on the mica substrate which have an average height of 2.9 ± 0.4 nm. The image lateral dimensions are $3 \times 3 \mu\text{m}$. (b) Atomic force microscopy height images of T-PS211k polystyrene nanoparticles on the Sigmacote substrate which have an average height of 9.3 ± 1.7 nm. The image lateral dimensions are $3.5 \times 3.5 \mu\text{m}$. (c) Should the nanoparticles adopt a spherical conformation on the substrate, then their height (H) should equal their diameter (D) which is 8.6 nm for the T-PS211k system (see Table 1). The nanoparticles may adopt a deformed shape on the substrate of equal volume to the sphere with a contact diameter d as described by the JKR theory.

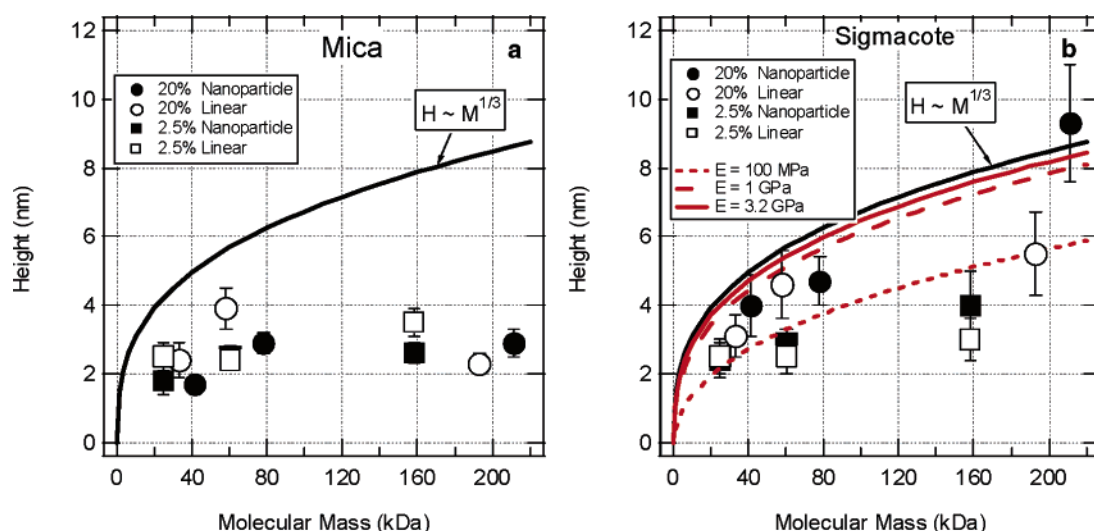


Figure 3. Height variation of lightly and tightly cross-linked nanoparticles (with different molecular weights) on substrates of high (a) and low (b) surface free energy. The height values measured on the mica surface are much less than the predicted value, eq 1 (curve labeled $H \sim M^{1/3}$), whereas the values measured on the Sigmacote surface approach the prediction of a spherical object for the tightly cross-linked nanoparticles. Height variation for three different moduli on the low-energy substrates is also shown (eq 6).

Table 1, and for sample T-PS211k, shown in Figure 2, the value of D (8.6 nm) is much greater than its height on the high-energy substrate (the average height is 2.9 ± 0.4 nm). Thus, on the mica surface the nanoparticles adopt a pancake-like conformation. This pancake-like conformation is also observed in dendrimer structures. Studies have shown that both charged and uncharged dendrimers adsorb to a mica surface forming a flat disk structure.⁸ Note the surface free energy of the mica is dependent on its environment which has a value of ~ 4500 mN/m in high vacuum and ~ 300 mN/m in humid laboratory air.⁹

To ensure that the height was not an AFM artifact, and caused by the cantilever drive amplitude (force), the amplitude was changed from 900 to 1500 mV when examining the T-PS211k nanoparticle sample. There was no change in the average nanoparticle height due to the equivalent pressure change, and therefore, it is suspected the high surface free energy mica (~ 300 mN/m) is the most likely cause for the nanoparticles' collapse onto the surface. The setpoint did not

play a role in these observations because the lowest possible setpoint was used for all AFM scans.

The effect of surface free energy on the nanoparticle conformation is shown in Figure 3 and it is clear that the nanoparticles' height is affected. The solid line in each graph, labeled $H \sim M^{1/3}$, is a plot of eq 1 assuming the density is equal to that for bulk polystyrene. The height of the linear precursor macromolecules and lightly cross-linked nanoparticles are affected little by a change in the surface free energy and fall below the value for a robust sphere. However, the tightly cross-linked nanoparticles show a drastic difference in the height profile with molecular mass and approach the scaling suggested by eq 1 on the low-energy substrate, Sigmacote. So, there is a clear interaction between the substrate surface free energy and nanoparticle stiffness implied through the degree of cross-linking.

Since the T-PS series of nanoparticles collapses on the high energy mica substrate, a system was designed to ensure minimal collapse on any energy surface. This was done by

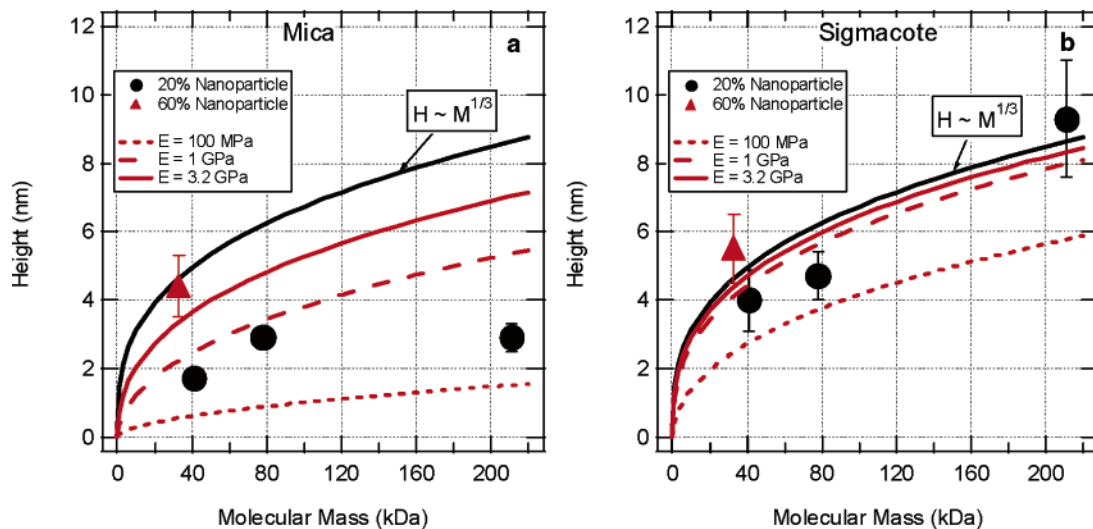


Figure 4. Height variation of two different cross-linked PS nanoparticles (20% and 60%), corresponding to the T-PS and E-PS systems, on high- and low-energy substrates. It can be seen that the E-PS system does not change shape on the high-energy (a) or low-energy (b) substrate within experimental error. Height variation for three different moduli on the high and low free energy substrates is also shown (eq 6). A modulus of 3.2 GPa is the calculated modulus for the extremely cross-linked system using eq 8 as described in the text.

recognizing the work of Chubynsky and Thorpe¹⁰ who show a rigid network system is developed when the average coordination number ($\langle r \rangle$), determined through

$$\langle r \rangle = 2x_L + 3[1 - x_L] \quad (2)$$

is 2.4 in a cross-linked system. Here x_L is the mole fraction of linear segments with coordination number 2 and $1 - x_L$, the mole fraction of cross-linked sites with coordination number 3. According to this theory, at least 40 mol % cross-linking, or two of every five monomer units, must be cross-linked to ensure rigidity. We designed the extremely cross-linked system to surpass this value with $\langle r \rangle = 2.6$ where three of every five monomer units are cross-linked.

The extremely cross-linked nanoparticles were observed on both the high and low surface free energy substrates and as shown in Figure 4 the nanoparticles do not change shape, within experimental error, on the high-energy substrate. The experimental error observed in both Figures 3 and 4 could be due to the nanoparticle's polydispersity index (PDI) affect on the height. For the E-PS33k polystyrene nanoparticle series, it is found that the change in height based on PDI is 1.5 nm,¹¹ which could contribute to the AFM height's experimental error of 1 nm. For reference, the T-PS series is also shown in Figure 4 and it is clear that these nanoparticles are distorted on the high energy substrate.

This result demonstrates that an extremely large degree of cross-linking is necessary to stabilize polymeric nanoparticles on the high-energy substrates suggesting a high modulus is required. Modeling of the linear polymer and nanoparticle conformation on the substrate can be achieved using the classic JKR theory¹² and the assumption that the adsorbate geometry adopts a spherical cap shape (Figure 2c). The JKR theory is an extension of the Hertz theory of elastic contact and is used to explain the adhesion between two elastic bodies under a compressive force. In the JKR theory it is assumed that elastic deformation must occur; however,

studies performed by Kendall and Padgett have shown that the JKR theory applies to the coalescence behavior of latex particles even though large deformations are present and the material is not truly elastic.¹³ Given this observation, we use the JKR theory for a sphere in contact with a flat surface, experiencing zero load, where the contact diameter (d) becomes

$$d^3 = 9\pi(1 - \nu^2) \frac{W_A}{E} D^2 \quad (3)$$

with D being the predicted nanoparticle diameter (eq 1), E is Young's modulus, ν is Poisson's ratio, and W_A is the work of adhesion given by

$$W_A = \gamma_A + \gamma_S - \gamma_{A/S} \approx 2(\gamma_A^d \gamma_S^d)^{1/2} \quad (4)$$

with γ being the surface free energy of the adsorbate–vapor (A), substrate–vapor (S), and adsorbate–substrate (A/S) interfaces. The approximation is due to Fowkes' relation¹⁴ that is applicable to lower energy substrates that interact through dispersive forces (the superscript d represents the dispersive part of the surface free energy or tension). In our case, polystyrene¹⁵ interacts via dispersive forces and has $\gamma_A^d = 40$ mN/m while the silanized substrate has $\gamma_S^d \approx 28.6 \pm 0.6$ mN/m at room temperature. Note there appears to be an error in the Kendall–Padgett work and the numerical factor in eq 3 should be 9 and not 18.

As stated above, the adsorbate geometry is assumed to be a spherical cap and with equal (constant) density between the spherical shape (see eq 1) and the adsorbed shape (see Figure 2c) one finds

$$d^3 = \frac{8}{3\sqrt{3}} \frac{(D^3 - H^3)^{3/2}}{H^{3/2}} \quad (5)$$

where H is the adsorbate's height on the substrate. Combining the JKR theory and the spherical cap model, one can determine the interrelation between the nanoparticle height and surface and molecular properties

$$H^3 + kH - D^3 = 0 \quad (6)$$

where

$$k = \left[\frac{27\pi\sqrt{3}}{8} (1 - \nu^2) \frac{W_A}{E} D^2 \right]^{2/3}$$

By solving for H , with varying D , we were able to generate height–molecular weight relations for different modulus values as shown in Figure 3. Note that this model only corresponds to the nanoparticles and linear precursors that have not collapsed.

The E-PS series can be further investigated since these nanoparticles apparently minimally collapse on the low- and high-energy surfaces. Due to this phenomenon we can assume $D \approx H$ and therefore $[D - H] \rightarrow 0$. Using eq 6 and the assumed limit, H can be expressed as

$$H = D \left[1 - \frac{C}{C_r^{2/3}} \right] \quad (7)$$

where

$$C_r = \frac{ED}{W_A(1 - \nu^2)} \quad \text{and} \quad C = \left(\frac{9\pi}{8} \right)^{2/3}$$

The term C_r in eq 7 refers to the crumble number, which was developed by Kendall and Padgett, to serve as a guideline for the coalescence behavior of dispersed elastic particles. The crumble number can be used to determine if a latex film will become porous and opaque ($C_r > 10$) or if the system will become tough, transparent, and nonporous ($C_r < 1$).¹³ Using this expression for the two substrates (labeled 1 and 2 for mica and Sigmacote), one finds

$$\frac{H_2 - H_1}{D} = -C \left[\frac{1}{C_{r2}^{2/3}} - \frac{1}{C_{r1}^{2/3}} \right] \quad (8)$$

Assuming $\nu = 0.5$, then the modulus is the only unknown parameter and we find $E \approx 3.2$ GPa. It is shown in Figure 4 that a model curve with a modulus of 3.2 GPa corresponds well with the height value for the E-PS series on either substrate. Further, the modulus for the E-PS series proves to be approximately equal to that for bulk polystyrene (≈ 3 GPa), traditionally determined with tensile testing or with AFM.¹⁶ This may be expected due to the extreme degree of cross-linking, yet the system is a single molecule and hence may be subject to finite size effects.

We can also estimate the modulus for T-PS nanoparticles by noting that they minimally collapse on the low-energy substrate. Assuming $C_r > 10$ for this system (eq 7) we

estimate $E > 100$ –150 MPa, where in fact we find $E = 1$ GPa agrees fairly well with the height data (Figure 4). Thus, increasing the degree of cross-linking by 3-fold produces a change in the modulus by about a half-order of magnitude.

The L-PS and T-PS, as well as the linear precursor polymers collapse on the substrates, particularly on the high-energy mica. To understand why their height becomes so small (≈ 3 nm) and essentially independent of molecular weight, we consider the work of Rubinstein and co-workers who have studied single chain adsorption on surfaces,¹⁷ with an intent to study the adsorption of polyelectrolytes on charged surfaces.^{18,19} If the surface is weakly adsorbing, then the number of monomer units in contact with the surface will increase in order to gain adsorption energy; therefore, the chain height on the substrate will be smaller than its unperturbed size and lose conformational entropy. This phenomenon is observed on the mica substrate for the L-PS and T-PS nanoparticle systems where the number of monomer units within the nanoparticle that are in contact with the surface must increase causing the nanoparticles to spread out onto the surface into a pancake-like conformation. The size of the adsorption blob (ξ_{ads}), which is equivalent to the chain height on the substrate, can be estimated by knowing the number of monomers in each adsorption blob that are in contact with the surface and each individual adsorption blob's energy gain estimated through

$$\delta k_B T \left(\frac{\xi_{\text{ads}}}{b} \right)^{2/3} \approx k_B T \quad (9)$$

where $\delta k_B T$ is the thermal energy gain of each individual monomer in contact with the surface. Here b represents the Kuhn monomer length, which is 1.8 nm for polystyrene. Assuming $\xi_{\text{ads}} \approx H$, one can find the adsorption energy per monomer for a linear polymer or collapsed nanoparticle ($H \approx 3$ nm, see Figure 3) to be $\approx 0.5 k_B T$. Since dispersion forces are $\approx k_B T$ in strength, this estimate of the adsorption blob–substrate interaction energy is expected as is the adsorbate conformation.

The factors necessary to ensure nanoparticles exhibit minimal collapse on selected substrates are described above. After investigation of the interaction between nanoparticles and a low- and high-energy substrate, it was determined that the conformation of nanoparticles changes significantly. It was discovered that the L-PS and T-PS series collapse forming a pancake-like conformation on a high-energy substrate with an adsorption energy adequately described by a theory developed for linear polymer systems. Conversely, on the low-energy substrate, the T-PS and E-PS series form robust spherical objects with a height that corresponds to their molecular weight. Yet, the modulus is estimated to be a half-order of magnitude larger for the E-PS system. Further, only the E-PS molecule does not significantly collapse on either substrate demonstrating an extremely rigid network is required for the nanoparticle to retain its shape regardless of substrate surface free energy. Since the motivation for this work requires a deformable nanoparticle, it is clear that extreme cross-linking cannot be used and so the interplay

of substrate surface free energy and nanoparticle modulus must be carefully considered.

Acknowledgment. Funding from the National Science Foundation under the NIRT program, Grant No. 0210247, small equipment grant scheme to purchase the light scattering detector system, Grant No. 0417640, and Michigan State University (M.E.M.) are gratefully acknowledged. We also thank Pacific Nanotechnology for their help with the AFM instrument and one of the reviewers for very pertinent comments which helped this work.

References

- (1) Vettiger, P.; Cross, G.; Despont, M.; Drechsler, U.; Dürig, U.; Gotsmann, B.; Häberle, W.; Lantz, M. A.; Rothuizen, H. E.; Stutz, R.; Binnig, G. K. *IEEE Trans. Nano.* **2002**, *1*, 39–55.
- (2) Harth, E.; Van Horn, B.; Lee, V. Y.; Germack, D. S.; Gonzales, C. P.; Miller, R. D.; Hawker, C. J. *J. Am. Chem. Soc.* **2002**, *124*, 8653.
- (3) Zhang, Q.; Clark, C. G.; Wang, M.; Remsen, E. E.; Wooley, K. L. *Nano. Lett.* **2002**, *2*, 1051–1054.
- (4) Richardson, M. J. *J. Polym. Sci.: Part C* **1965**, *3*, 21.
- (5) Israelachvili, J. N.; Alcantar, N. A.; Maeda, N.; Mates, T. E.; Ruths, M. *Langmuir* **2004**, *20*, 3616.
- (6) Ebenstein, Y.; Nahum, Eyal; Banin, Uri. *Nano. Lett.* **2002**, *2*, 945.
- (7) Markiewicz, P.; Goh, M. C. *Langmuir* **1994**, *10*, 5.
- (8) Mecke, A.; Lee, I.; Baker, J. R., Jr.; Banaszak, Holl, M. M.; Orr, B. G. *Eur. Phys. J. E* **2004**, *14*, 7.
- (9) Israelachvili, J. *Intermolecular & Surface Forces*; Academic Press: London, 1992; p 314.
- (10) Chubynsky, M. V.; Thorpe, M. F. *Curr. Opin. Solid State Mater. Sci.* **2001**, *5*, 525.
- (11) For a polydisperse system the molecular weight standard deviation (δM) is given by $M_n \times \sqrt{(\text{PDI}-1)}$ which can be used to calculate the error in the diameter (δD); $\delta D/D = \delta M/3M$, through propagation of error.
- (12) Johnson, K. L.; Kendall, K.; Roberts, A. D. *Proc. R. Soc. London, Ser. A* **1971**, *324*, 301.
- (13) Kendall, K.; Padget, J. C. *Int. J. Adhes. Adhes.* **1982**, *2*, 149–154.
- (14) Fowkes, F. M. *Ind. Eng. Chem.* **1964**, *56*, 40–52.
- (15) Dee, G. T.; Sauer, B. B. *Colloid Interface Sci.* **1992**, *152*, 85–103.
- (16) Ferry, J. D. *Viscoelastic properties of polymers*, 3rd ed.; J. Wiley & Sons: New York, 1980.
- (17) Rubinstein, M.; Colby, R. H. *Polymer Physics*; Oxford University: New York, 2003; pp 104–113.
- (18) Dobrynin, A. V.; Deshkovski, A.; Rubinstein, M. *Phys. Rev. Lett.* **2000**, *84*, 3101.
- (19) Dobrynin, A. V.; Rubinstein, M. *Macromolecules* **2002**, *35*, 2754.

NL050941F